ARCHIVES OF ELECTRICAL ENGINEERING VOL. 67(1), pp. 95–108 (2018)

DOI 10.24425/118994

FPGA-based control of output voltage of SRG drive system

ADAM POWRÓZEK

Faculty of Electrical and Computer Engineering, Rzeszow University of Technology
Wincentego Pola 2, 35-959 Rzeszów, Poland
e-mail: apow@prz.edu.pl

(Received: 10.08.2017, revised: 22.10.2017)

Abstract: The paper presents an FPGA-based output voltage control system of a four-phase switched reluctance generator above base speed. The presented control strategy uses a digital PI controller to vary turn-off angle at fixed turn-on angle under single-pulse mode. Simulation tests were conducted based on the simulation model built in the Matlab/Simulink environment. The results of the simulation and laboratory tests as waveforms of voltages and currents are presented. Based on the presented control system, the dependencies of overall efficiency in the function of turn-on angle and ratio of output power to rms phase current ($P_{\text{out av}}/I_{\text{ph rms}}$) in the function of turn-on angle were determined. They allow for the selection of a proper value of turn-on angle for the optimal performance of the generator during the output voltage control. The results obtained from laboratory and simulation tests are discussed in the conclusions.

Key words: switched reluctance generator, single-pulse mode, output voltage control, FPGA-based control

1. Introduction

Switched reluctance machines (SRM) are categorized among machines with an electronic commutation. Their merits include: simple rotor structure (no windings or permanent magnets) and therefore low production cost, wide speed range, high-temperature operation and high reliability [1]. By proper selection of control angles (turn-on and turn-off angles), SRM can operate as a motor or as a generator. However, there are some important differences in control and controller design when high performance is required. The switched reluctance generator (SRG) is under development for applications that include: hybrid electric vehicles, aerospace and wind turbines [2–4]. In some applications, both motoring and generating operation is required. We can consider the integrated starter/generator as an example [5].

The control of the SRM is more complicated for generator operation than it is for motor operation. Moreover, it is also more complicated compared to other types of machines. The control

of the SRG is typically performed by DSPs [6–7]. However, DSPs cannot be fast enough to meet timing specifications because control of SRG requires a high accuracy of rotor position detection and novel control algorithms require fast computation update rate [8–9]. Thus, field programmable gate arrays (FPGA) have recently become an alternative solution for the realization of electric machines control systems [10–13]. An FPGA is defined as a matrix of configurable logic blocks which are linked to each other by an interconnection network which is entirely reprogrammable. FPGAs have highly configurable pins which allow the flexible pin assignment and they are able to meet the specific electric machine control requirements. The scalability of hardware within the FPGA is greater than a DSP due to its ability to replicate hardware multiple times throughout the chip, which is limited only to the size of the FPGA [8]. The block design of the controller allows the designer to construct the controller in a modular way and each block can run independently because of the parallel nature of the FPGA. Therefore, the FPGA is a fully customizable to the requirements of the designers. Compared with languages used by DSPs or microcontrollers, the VHDL or the Verilog which are used to program FPGAs are independent of devices and manufactures. Therefore, they can be compatible with different platforms and can be synthesized into any FPGA without major changes. FPGAs have also disadvantages: they need many resources for complex mathematical operations since they are not arithmetically-oriented like DSPs. Thus, a connection of the DSP with the FPGA can be a solution for applications where control functions are divided between the DSP and the FPGA [14–15]. The designer can also take advantage in remodelling the target algorithm in order to reduce the number of operations to be implemented. Therefore, smart solutions should be taken to avoid including greedy operators like dividers in their designs. Development times are usually longer in the FPGA due to an extra step which is required to design the hardware within the chip.

The one of the objectives of the SRG control is to keep the output voltage at a desired value and it is not possible without a proper control algorithm. Therefore, the control angles should be changed according to the speed of the prime mover, output voltage and power requirements of the load. SRG output voltage control systems without analysing performance of the generator are presented in [12] and [16]. However, control angles should be adjusted online to obtain optimal performance of the SRG e.g. operation with high efficiency or high ratio of output power to rms phase current. Below base speed, the controller can regulate control variables, such as, current level, turn-on angle and turn-off angle. On the other hand, above base speed, a current regulation is not possible and control angles are the only control variables (single-pulse mode). What is more, this is more challenging for generation operation because peak phase current for the SRG occurs when both switches in a power converter are off. In the paper [17], authors present through simulations the optimal variation of turn-on angle and turn-off angle under minimized excitation penalty, RMS current, peak phase current or peak flux-linkage above base speed. The simple equations for optimal control angles for high-efficiency operation based on the optimal control of flux-linkage are proposed in [18].

This paper presents an FPGA-based output voltage control system of a four-phase SRG above base speed. The control method uses a digital proportional-integral (PI) controller to regulate turn-off angle (with fixed turn-on angle) in the single-pulse mode. The complete system is implemented by dividing system functions into reconfigurable modules. The control method was verified in simulation and laboratory tests and waveforms of voltages and currents were presented. The simulation tests were developed based on the nonlinear simulation model that was

built in the Matlab/Simulink environment. Based on the presented control system, the dependencies of overall efficiency in the function of turn-on angle and ratio of output power to rms phase current $(P_{\text{out av}}/I_{\text{ph rms}})$ in the function of turn-on angle were determined. They allow selecting a proper value of turn-on angle for optimal performance of the generator during the output voltage control.

2. Output voltage control of SRG

The subject of the simulation and laboratory tests is a four-phase 8/6 switched reluctance machine with basic parameters listed in Table 1.

Table 1. Basic parameters of the SRM

Machine type	**SRM**
Number of phases	4
Number of stator/rotor poles	8/6
Rated supply voltage	24 V
Rated power	750 W
Rated speed	3000 rpm

A four-phase SRG converter (the H-type half-bridge) with two controlled power switches and two diodes per phase which source a resistive load was used in the tested machine. Fig. 1 shows a scheme of the SRG converter system.

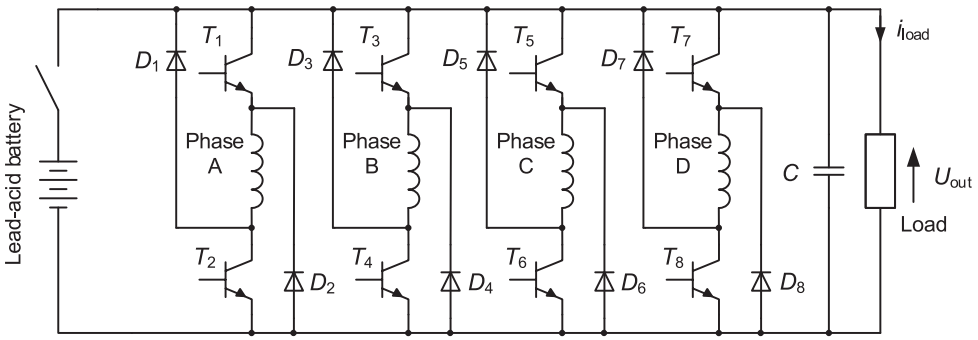

Fig. 1. A schematic diagram of the SRG converter system

A lead-acid battery of 12 V rated voltage is used as an excitement source (to initiate the generating operation). The battery is only used to initiate first excitement of the SRG (charge a capacitor C). After the first excitement from the lead-acid battery, the generator operates in the self-excitation mode. The capacitor C is chosen large enough to assure fairly constant output voltage at each stroke.

In generating operation of the SRM, when both switches in each phase are on, the SRG obtains its excitation from the same dc bus that it supplies power to after the both switches are turned off. The SRG has the tendency of being open-loop unstable, so a closed-loop control is required to stabilize the system. The one of the objectives of the SRG control is to keep the output voltage at a desired value and above base speed output voltage can be controlled by changing control angles in single-pulse mode or by changing average value of excitement voltage (by changing PWM value) [12]. The classic current regulation is not possible above base speed because the back-electromotive force (back-EMF) is higher than the dc-link voltage (U_{out}). However, in paper [19], the author proposed a novel method of controlling the current under a generator operation of SRM under single-pulse mode. It was called the generator dependent current control (GDCC) in which the current controller in the outgoing phase depends on the current controller in the present phase.

Fig. 2 shows a schematic diagram of an output voltage control method where a digital PI controller varies the width of the magnetization period by changing the value of turn-off angle θ_{off} with fixed turn-on angle θ_{on}. In both simulation and laboratory tests, the digital PI controller (with backward Euler) with the following equation was used:

$$u[k] = u[k-1] - Ke[k-1] + K\frac{T_s}{T_i}e[k], \tag{1}$$

where: $u[k]$ is the control variable, $u[k-1]$ is the previous control variable, e is the error, $e[k-1]$ is the previous error, T_s is the sampling time, T_i is the integral time, K is the proportional gain.

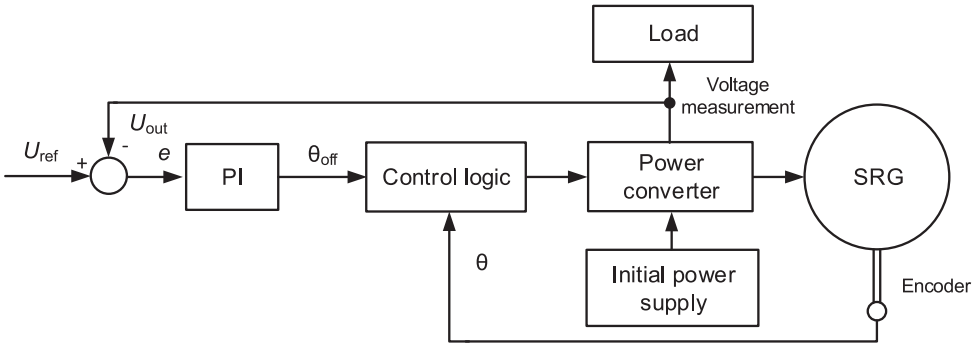

Fig. 2. A schematic diagram of the output voltage control method

To check whether the control system works properly, a value of turn-on angle θ_{on} was selected at random in both simulation and laboratory tests. A complex FPGA-based control system with optimal performance of the SRG (e.g. high-efficiency, high ratio $P_{\text{out av}}/I_{\text{ph rms}}$) where both control angles are adjusted online will be a subject of future research. The control system keeps the output voltage at a level of 14.4 V which is a standard electrical system in most automobiles [4]. A measured output voltage U_{out} is compared with a reference value U_{ref} and error e is directed to the PI controller which varies the value of turn-off angle θ_{off}.

3. Simulation tests

3.1. The simulation model

The nonlinear simulation model of the SRG was built in the Matlab/Simulink environment. It was realized based on the mathematical model presented in [1]. The following assumptions were taken into account in the simulation model:

– negligibly small couplings between phases,
– magnetic circuit may operate in saturation region,
– negligible core losses.

The measured current-angle-flux and torque-current-angle characteristics were implemented in *Look-Up Table* blocks and they were presented in Fig. 3. The SimPowerSystems library was used to build a power converter. Fig. 4 shows the block diagram of the power converter for a four-phase SRG.

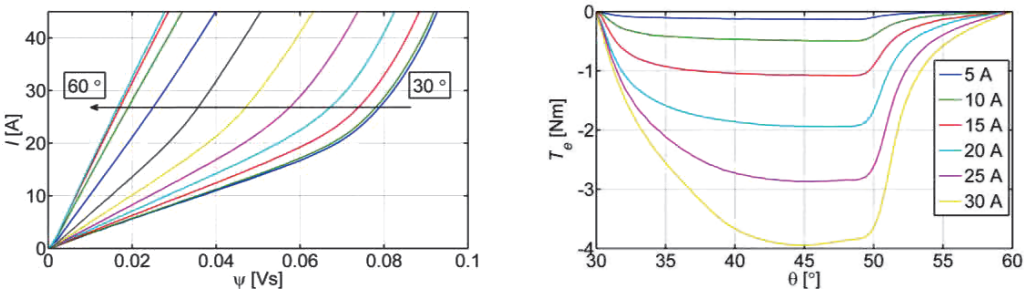

(a) (b)

Fig. 3. Characteristics: (a) $i = f(\theta, \psi)$; (b) $T_e = f(\theta, i)$

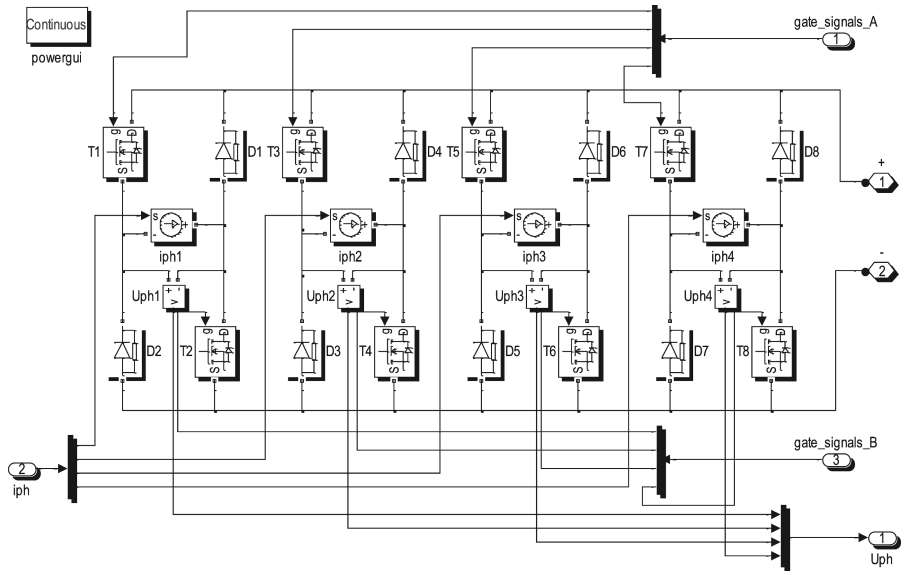

Fig. 4. SRG power converter

Fig. 5 shows a simulation model of the SRG drive. The model is divided into three main blocks, i.e. the *SRG*, the *Power converter* and the *Control module* in which control logic was implemented. The initial voltage (for first excitement) was set in the capacitor *C* block.

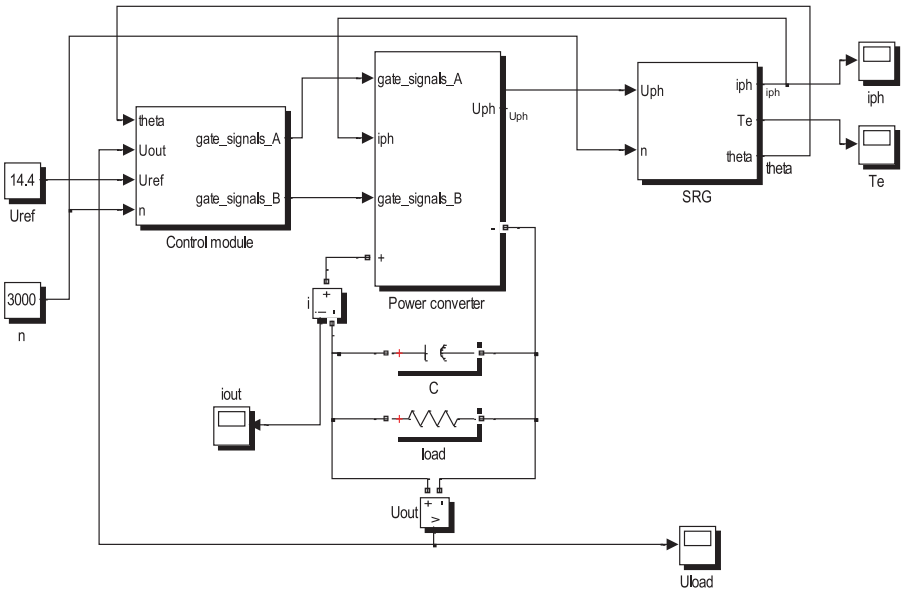

Fig. 5. A simulation model of the SRG drive

3.2. Output voltage control

The simulation tests of the output voltage control method were performed in two variants:

– step change of load at constant speed,
– speed variation at constant load.

In the first variant, tests were conducted at a fixed rotor speed of 3000 r/min. The machine was simulated during 1.8 seconds. At time $t = 0.4$ s a load was changed from 2.9 Ω to 1.9 Ω while at time $t = 1.2$ s the load was changed from 1.9 Ω to 2.9 Ω. A reference voltage was set to $U_{\text{ref}} = 14.4$ V and turn-on angle was set to $\theta_{\text{on}} = 23^\circ$ (it was assumed that 0° point is in the position where phase inductance is minimum). Fig. 6 shows the behaviour of output voltage U_{out} and load current i_{load} during the simulation period.

It is verified through simulation tests that the set reference voltage (14.4 V) was properly maintained. The voltage fluctuation is about ±0.5 V and the recovery time is about 20 ms. These results show that the control loop is able to keep the generated output voltage in the set value, despite the sudden load change. Fig. 7 shows a waveform of one phase current during the simulation period.

In the second variant, simulation was conducted at a constant load of 1.9 Ω with variable speed. The machine was simulated during 8 seconds. A reference voltage was set to $U_{\text{ref}} = 14.4$ V and turn-on angle was set to $\theta_{\text{on}} = 23^\circ$. Fig. 8 shows waveforms of output voltage U_{out} and a trajectory of speed n during simulation.

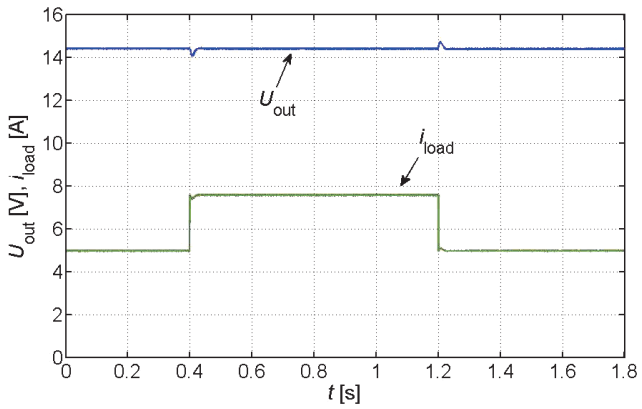

Fig. 6. Waveforms of output voltage U_{out} and load current i_{load} during step change of load at speed $n = 3000$ r/min and $\theta_{on} = 23^\circ$

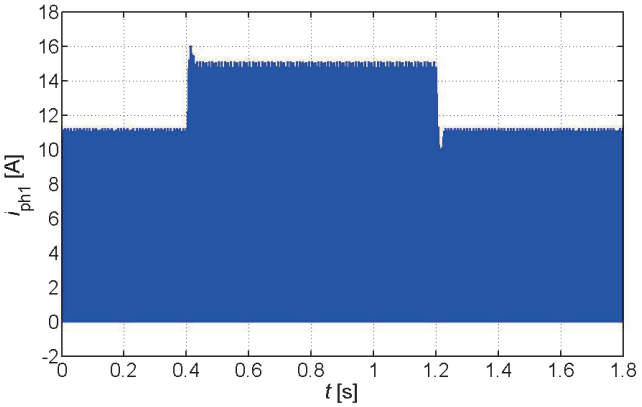

Fig. 7. Waveform of phase current i_{ph1} during step change of load at speed $n = 3000$ r/min and $\theta_{on} = 23^\circ$

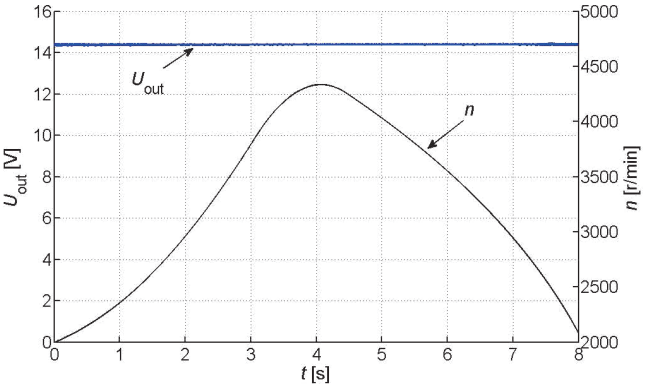

Fig. 8. Waveforms of output voltage U_{out} and speed n trajectory at constant load of 1.9 Ω; and fixed turn-on angle $\theta_{on} = 23^\circ$

Fig. 9 shows behaviour of one phase current i_{ph1} during the simulation period. It was also verified through simulations that the set reference voltage (14.4 V) was properly maintained during the entire range of speed variation. These results show that a closed-loop voltage controller is able to keep the generated output voltage in the set value, despite variation of the prime mover speed.

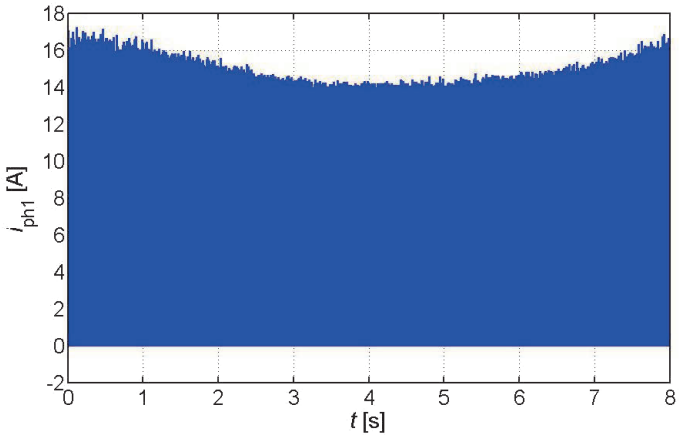

Fig. 9. Waveform of phase current i_{ph1} at constant load of 1.9 Ω and fixed turn-on angle $\theta_{on} = 23^\circ$ during speed variation

4. Laboratory tests

4.1. FPGA-based control system

The control system of the SRG was implemented using FPGA Spartan-3AN from Xilinx (XC3S700AN). The XC3S700AN contains 13248 LCs, 1472 CLBs and 372 user input/output blocks. The Xilinx ISE Webpack tool was used for the design and development of the FPGA. The Spartan-3AN board has a 50-MHz oscillator. The logic implemented in the FPGA is subdivided into different functional blocks representing Verilog entities. A schematic diagram of the FPGA-based control system was shown in Fig. 10. Most of the modules were synchronized with 50 MHz clock, the clock generator was used to generate SPI interface send clock (12.5 MHz) and PI controller clock (1500 Hz). They operate independently from one another due to the parallel nature of the FPGA.

The *ADC_controller* entity contains logic to read out the output voltage from AD7606. The AD7606 is a 16-bit 8-channel ADC with a conversion time of about 4 μs. The ADC send SPI interface was clocked at 12.5 MHz and information from the ADC is known every 10.7 μs. The information from the *ADC_controller* is compared with a reference value ($U_{ref} = 14.4$ V) and error e is directed to the *PI_controller* entity where the digital PI controller (based on Equation (1)) is implemented. The *encoder_controller* entity contains logic, which specifies the actual rotor position. Moreover, it calculates the speed of the generator. A 720-pulse incremental encoder was

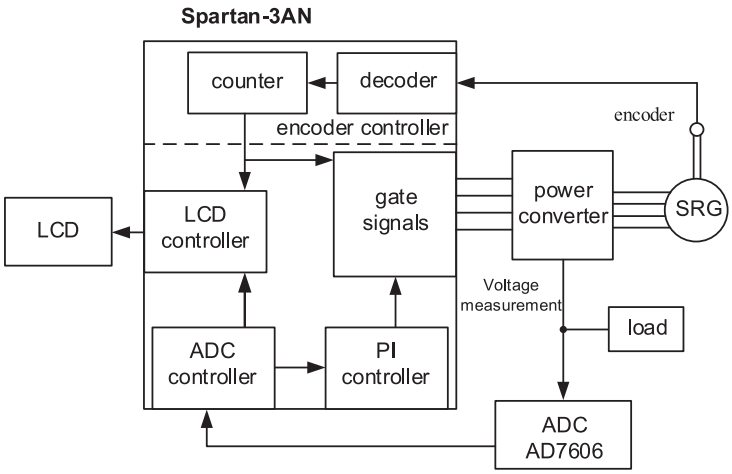

Fig. 10. A schematic diagram of FPGA-based control system

used and it was mounted on the generator shaft. The detection of all four slopes of encoder signals gives a resolution of 0.125°. Based on the information from the *encoder_controller* entity and from the *PI_controller* entity, the *gate_signals* entity generates gate signals of transistors in the power converter.

4.2. Output voltage control

The laboratory setup was developed to verify the simulated results. Fig. 11 shows a block diagram of the laboratory setup which consists of the SRG (with details listed in Table 1) and a prime mover (an induction motor) with a power of 2.2 kW. The induction machine was supplied from a frequency inverter. Fig. 12 shows a view of the laboratory setup.

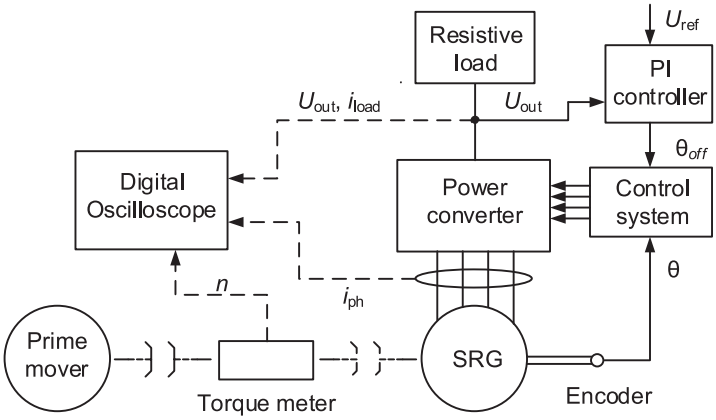

Fig. 11. A block diagram of the laboratory setup

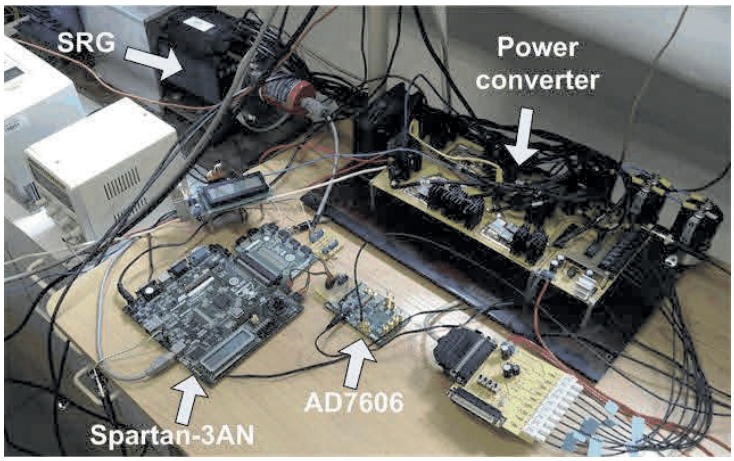

Fig. 12. The laboratory setup

The laboratory tests were also performed in two variants (step change of load with fixed speed and variation of speed with a fixed load). A reference value of output voltage was set to 14.4 V. Fig. 13 shows waveforms of output voltage U_{out}, phase current i_{ph1} and load current i_{load} during step change of load (from 2.9 Ω to 1.9 Ω and from 1.9 Ω to 2.9 Ω) at speed $n = 3000$ r/min and $\theta_{\text{on}} = 23°$.

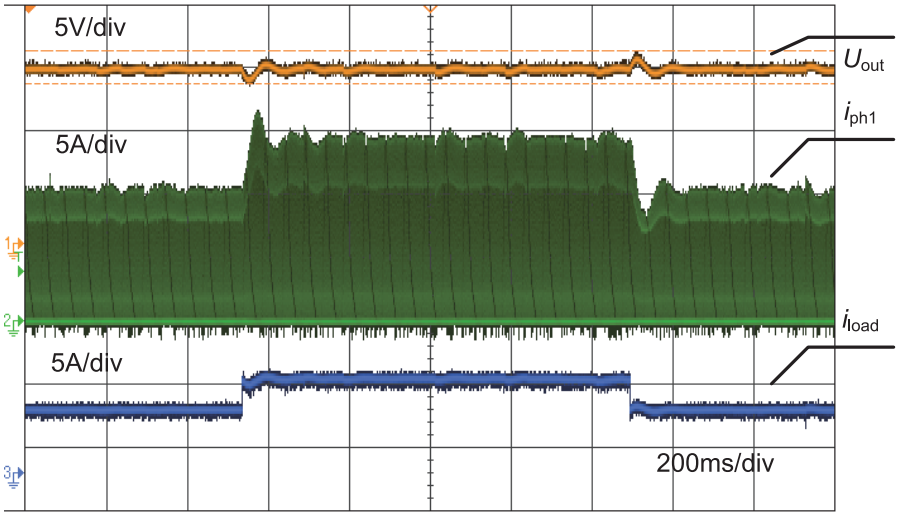

Fig. 13. Waveforms of output voltage U_{load}, phase current i_{ph1}, load current i_{load} during step change of load at speed $n = 3000$ r/min and $\theta_{\text{on}} = 23°$

These results show that the controller is able to maintain the generated voltage U_{out} in the set value, despite the sudden change of load. In the second test, the behaviour of the SRG was

verified under speed variation. The SRG was accelerated from 2000 r/min to 4000 r/min and then it was decelerated from 4000 r/min to 2000 r/min. Fig. 14 shows waveforms of output voltage U_{out}, speed n, phase current i_{ph1} and load current i_{load} during acceleration and deceleration. It can be seen that the output voltage remained at the reference value.

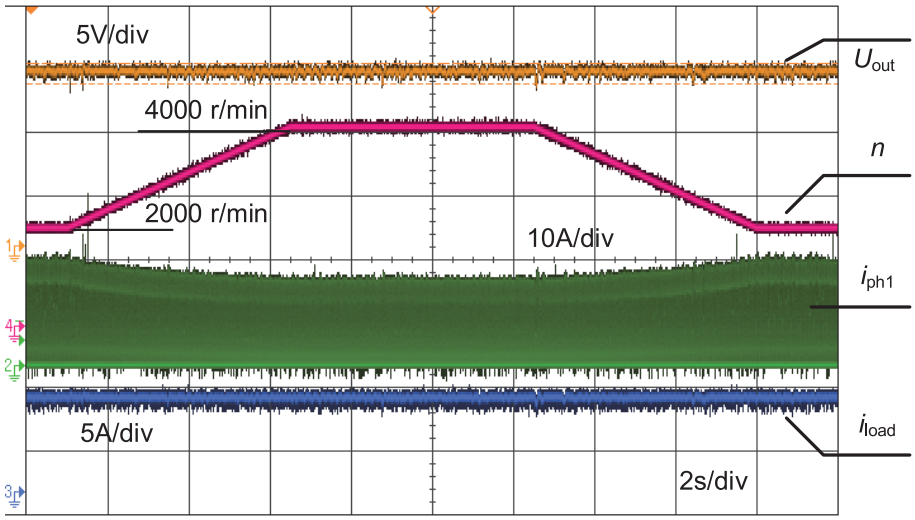

Fig. 14. Waveforms of output voltage U_{load}, speed n, phase current i_{ph1}, load current i_{load} during speed variation at fixed load 1.9 Ω and $\theta_{\text{on}} = 23°$

4.3. Defining the optimal turn-on angle

During the operation of an SRM as a generator, both turn-on and turn-off angles control the peak phase current so the selection of the best excitation parameters is an important issue [17, 18]. Therefore, the optimal SRG performance (e.g. high-efficiency, high ratio of output power to rms phase current) can be obtained through turn-on and turn-off angles control, regarding to load requirements and depending on rotor speed and output voltage. Based on the FPGA-based output voltage control system presented in part 4.1, the dependencies of the overall efficiency in the function of turn-on angle and the ratio of output power to rms phase current $(P_{\text{out av}}/I_{\text{ph rms}})$ were determined during output voltage control at desired value (14.4 V) by changing of turn-off angle. The turn-on angle value was changed with a step of 0.5°. A Yokogawa WT1600 digital power meter was used to measure all electric (current, voltage and power) and mechanical (speed) parameters of the SRG.

Fig. 15 shows dependencies of ratio $P_{\text{out av}}/I_{\text{ph rms}}$ in the function of turn-on angle θ_{on} with marked points of maximum values at a load of 2.9 Ω, $U_{\text{out}} = 14.4$ V for various speeds (Fig. 15a) and at a load of 1.9 Ω, $U_{\text{out}} = 14.4$ V for various speeds (Fig. 15b). Fig. 16 shows dependencies of overall efficiency in the function of turn-on angle θ_{on} with marked points of maximum values at a load of 2.9 Ω, $U_{\text{out}} = 14.4$ V for various speeds (Fig. 16a) and at a load of 1.9 Ω, $U_{\text{out}} = 14.4$ V for various speeds (Fig. 16b). It can be seen in Fig. 16 that the efficiency is not high due to

lower operation voltage (14.4 V) than the rated value (24 V) and low load power (at 1.9 Ω $P_{\text{load}} = 108$ W and at 2.9 Ω $P_{\text{load}} = 72$ W). However, the purpose of the paper is to focus on the control method not on the machine for the specific application. The control method should adjust both control angles to obtain maximum efficiency which is available for given machine working point.

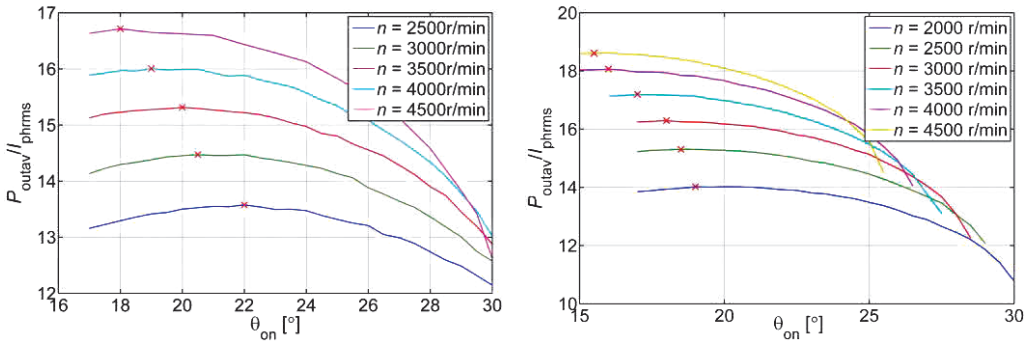

(a) (b)

Fig. 15. The ratio $P_{\text{out av}}/I_{\text{ph rms}}$ as a function of turn-on angle θ_{on} at $U_{\text{out}} = 14.4$ V and a load of: (a) 2.9 Ω and (b) 1.9 Ω

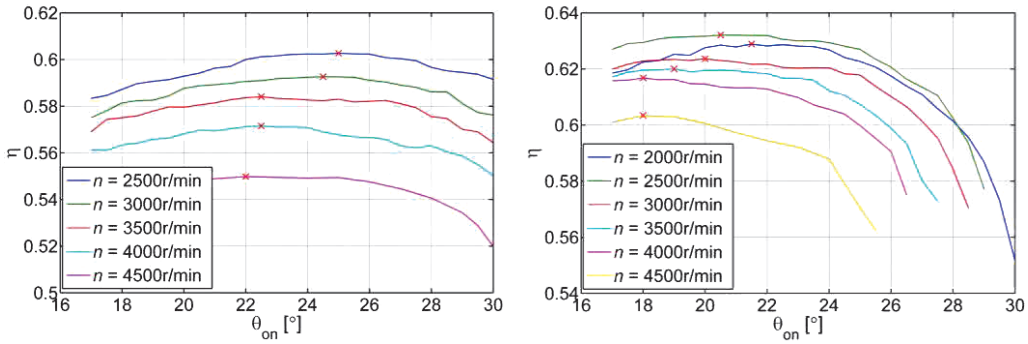

(a) (b)

Fig. 16. The overall efficiency η as a function of turn-on angle θ_{on} at $U_{\text{out}} = 14.4$ V and a load of: (a) 2.9 Ω and (b) 1.9 Ω

It can be seen in Figs. 15 and 16 that to obtain the highest ratio of $P_{\text{out av}}/I_{\text{ph rms}}$ and the highest efficiency, different values of turn-on angle should be selected. Therefore, the designer of the control system should decide which condition should be chosen. The analysis of optimal performance of the SRG will be continued in the future research to build a complex control system which will be adjusting online both control angles.

5. Conclusions

In the paper, the problem of output voltage control in single-pulsed controlled (above base speed) SRG drive was investigated. The output voltage control system of the SRG was implemented in the FPGA based on a digital PI controller which regulates turn-off angle at fixed turn-on angle. The FPGA-based control systems offer advantages such as a high speed (significantly reduced execution time), a complex functionality and a low power consumption. These are very attractive features from the point of view of embedded system design. The results of simulation tests which were carried out based on the nonlinear simulation model of the SRG were verified through experimental tests. The results of the experimental tests showed that the FPGA can be used in control of switched reluctance generators, where a fast and reliable control system is required. However, FGPAs need many resources for complex mathematical operations (like dividers) and the implementation of the PI controller and its tuning was hindered. The analysis of turn-on angle influence on overall efficiency and the ratio of $P_{\text{out av}}/I_{\text{ph rms}}$ during output voltage control with variation of turn-off angle showed that turn-on angle should be also online changed to obtain optimal performance of the SRG. Further research will be carried out to develop a complex control algorithm where both control angles will be online adjusted to obtain optimal performance of the SRG. Besides the presented dependencies, the other parameters like excitation penalty and peak phase current will be also taken into consideration.

References

[1] Miller T.J.E., *Electronic Control of Switched Reluctance Machines*, Newnes (2001).

[2] Rahmanian E., Akbari H., Sheisi G.H., *Maximum Power Point Tracking in Grid Connected Wind Plant by Using Intelligent Controller and Switched Reluctance Generator*, IEEE Transactions on Sustainable Energy, vol. 8, no. 3, pp. 1313–1320 (2017).

[3] Urase K., Yabu N., Kiyota K., Sugimoto H., Chiba A., Takemoto M., Ogasawara S., Hoshi N., *Energy Efficiency of SR and IPM Generators for Hybrid Electric Vehicle*, IEEE Transactions on Industry Applications, vol. 51, no. 4, pp. 2874–2883 (2015).

[4] Boldea I., Tutelea L.N., Parsa L., Dorrell D., *Automotive Electric Propulsion Systems With Reduced or No Permanent Magnets: An Overview*, IEEE Transactions on Industrial Electronics, vol. 61, no. 10, pp. 5696–5711 (2014).

[5] Ze Q., Kou P., Liang D., Liang Z., *Fault-tolerant performances of switched reluctance machine and doubly salient permanent magnet machine in starter/generator system*, 17th International Conference on Electrical Machines and Systems (ICEMS), Hangzhou, China, pp. 3417–3423 (2014).

[6] Nasirian V., Kaboli S., Davoudi A., *Output Power Maximization and Optimal Symmetric Freewheeling Excitation for Switched Reluctance Generators*, IEEE Transactions on Industry Applications, vol. 49, no. 3, pp. 1031–1042 (2013).

[7] Sikder Ch., Husain I., Sozer Y., *Switched Reluctance Generator Control for Optimal Power Generation with Current Regulation*, IEEE Transactions on Industry Applications, vol. 50, no. 1, pp. 307–316 (2013).

[8] Stumpf A., Elton D., Devlin J., Lovatt H., *Benefits of an FPGA based SRM controller*, Industrial Electronics and Applications (ICIEA), Hangzhou, China, pp. 12–17 (2014).

[9] Menghal P.M., Jaya Laxmi A., *Real time control of electrical machine drives: a review*, Power, Control and Embedded Systems (ICPCES), Allahabad, India, pp. 1–6 (2010).

[10] Monmasson E., Bahri I., Idkhajine L., Maalouf A., Naouar W.M., *Recent advancements in FPGA-based controllers for AC Drives Applications*, 13th International Conference on Optimization of Electrical and Electronic Equipment (OPTIM), Brasov, Romania, pp. 8–15 (2012).

[11] Dwijasish D., Kumaresan N., Nayanar V., Navin Sam K., Ammasai Gounden N., *Development of BLDC Motor-Based Elevator System Suitable for DC Microgrid*, IEEE/ASME Transactions on Mechatronics, vol. 21, no. 3, pp. 1552–1560 (2016).

[12] Silveira A.W.F.V., Andrade D.A., Fleury A.V.S., Gomes L.C., Bissochi C.A., Dias R.J., *Generated Voltage Control of the SRM operating as motor/generator*, Brazilian Power Electronics Conference, Bonito, Brasil, pp. 830–835 (2009).

[13] Tomczewski K., Wróbel K., *Improved C-dump converter for switched reluctance motor drives*, IET Power Electronics, vol. 7, no. 10, pp. 2628–2635 (2014).

[14] Stando D., Chudzik P., Moradewicz A., Miśkiewicz R., Kaźmierkowski M.P., *DSP-FPGA Based Computing Platform for Control of Power Electronic Converter*, Przegląd Elektrotechniczny, vol. 91, no. 12, pp. 1–6 (2015).

[15] Tarczewski T., Grzesiak L.M., Wawrzak A., Karwowski K., Erwiński K., *A state-space approach for control of NPC type 3-level sine wave inverter used in FOC PMSM drive*, Bulletin of the Polish Academy of Sciences Technical Sciences, vol. 62, no. 3, pp. 439–448 (2014).

[16] Guojun Y., Lei M., He C., Hao C., Yingjie H., *Research on the Control Strategy of Switched Reluctance Generator System*, International Power Electronics and Application Conference and Exposition, Shanghai, China, pp. 1242–1247 (2014).

[17] Fernando W.U.N., Barnes M., Marjanovic O., *Excitation Control and Voltage Regulation of Switched Reluctance Generators above Base Speed Operation*, IEEE Vehicle Power and Propulsion Conference, Chicago, USA, pp. 1–6 (2011).

[18] Kioskeridis I., Mademlis C., *Optimal Efficiency Control of Switched Reluctance Generators*, IEEE Transactions of Power Electronics, vol. 21, no. 4, pp. 1062–1072 (2006).

[19] Bogusz P., *The novel control method of switched reluctance generator*, Archives of Electrical Engineering, vol. 66, no. 2, pp. 409–422 (2017).